Environmental Loss Characterization of an Advanced Stirling Convertor (ASC-E2) Insulation Package Using a Mock Heater Head

Nicholas A. Schifer and Maxwell H. Briggs
Glenn Research Center, Cleveland, Ohio

NASA STI Program . . . in Profile

Since its founding, NASA has been dedicated to the advancement of aeronautics and space science. The NASA Scientific and Technical Information (STI) program plays a key part in helping NASA maintain this important role.

The NASA STI Program operates under the auspices of the Agency Chief Information Officer. It collects, organizes, provides for archiving, and disseminates NASA's STI. The NASA STI program provides access to the NASA Aeronautics and Space Database and its public interface, the NASA Technical Reports Server, thus providing one of the largest collections of aeronautical and space science STI in the world. Results are published in both non-NASA channels and by NASA in the NASA STI Report Series, which includes the following report types:

- TECHNICAL PUBLICATION. Reports of completed research or a major significant phase of research that present the results of NASA programs and include extensive data or theoretical analysis. Includes compilations of significant scientific and technical data and information deemed to be of continuing reference value. NASA counterpart of peer-reviewed formal professional papers but has less stringent limitations on manuscript length and extent of graphic presentations.

- TECHNICAL MEMORANDUM. Scientific and technical findings that are preliminary or of specialized interest, e.g., quick release reports, working papers, and bibliographies that contain minimal annotation. Does not contain extensive analysis.

- CONTRACTOR REPORT. Scientific and technical findings by NASA-sponsored contractors and grantees.

- CONFERENCE PUBLICATION. Collected papers from scientific and technical conferences, symposia, seminars, or other meetings sponsored or cosponsored by NASA.

- SPECIAL PUBLICATION. Scientific, technical, or historical information from NASA programs, projects, and missions, often concerned with subjects having substantial public interest.

- TECHNICAL TRANSLATION. English-language translations of foreign scientific and technical material pertinent to NASA's mission.

Specialized services also include creating custom thesauri, building customized databases, organizing and publishing research results.

For more information about the NASA STI program, see the following:

- Access the NASA STI program home page at *http://www.sti.nasa.gov*

- E-mail your question via the Internet to *help@sti.nasa.gov*

- Fax your question to the NASA STI Help Desk at 443–757–5803

- Telephone the NASA STI Help Desk at 443–757–5802

- Write to:
  NASA Center for AeroSpace Information (CASI)
  7115 Standard Drive
  Hanover, MD 21076–1320

Environmental Loss Characterization of an Advanced Stirling Convertor (ASC-E2) Insulation Package Using a Mock Heater Head

Nicholas A. Schifer and Maxwell H. Briggs
Glenn Research Center, Cleveland, Ohio

National Aeronautics and
Space Administration

Glenn Research Center
Cleveland, Ohio 44135

Acknowledgments

Environmental Loss Characterization of an Advanced Stirling Convertor (ASC-E2) Insulation Package Using a Mock Heater Head

Nicholas A. Schifer and Maxwell H. Briggs
National Aeronautics and Space Administration
Glenn Research Center
Cleveland, Ohio 44135

Abstract

The U.S. Department of Energy (DOE) and Lockheed Martin Space Systems Company (LMSSC) have been developing the Advanced Stirling Radioisotope Generator (ASRG) for use as a power system for space science missions. This generator would use two high-efficiency Advanced Stirling Convertors (ASCs), developed by Sunpower, Inc., and NASA Glenn Research Center (GRC). The ASCs convert thermal energy from a radioisotope heat source into electricity. As part of ground testing of these ASCs, different operating conditions are used to simulate expected mission conditions. These conditions require achieving a particular operating frequency, hot end and cold end temperatures, and specified electrical power output for a given net heat input. While electrical power output can be precisely quantified, thermal power input to the Stirling cycle cannot be directly measured. Traditionally, the environmental losses have been characterized based on testing a non-operating convertor. However, the thermal profile of a non-operating convertor does not adequately characterize the thermal profile of an operating convertor and, therefore, does not accurately predict net heat input. In an effort to improve net heat input predictions, numerous tasks have been performed which provided a more accurate value for net heat input into the ASCs, including testing validation hardware, known as the Mock Heater Head, to provide a direct comparison to numerical and empirical models used to predict convertor net heat input. The Mock Heater Head was primarily constructed of existing test hardware which had the same relative thermal paths as a convertor. The dominant conduction path is a removable rod that interfaces the interior dome of the Mock Heater Head. Two different diameter rods were used to vary the thermal load on the heater. While the rod and heater head cylinder wall provided conductive paths from the hot end to the cold end, the resulting thermal profile did not accurately simulate that of an operating convertor. The Mock Heater Head also served as the pathfinder for a higher fidelity version of validation test hardware, known as the Thermal Standard. This paper describes how the Mock Heater Head was tested and utilized to validate a process for the Thermal Standard through test configuration, instrumentation, calculations performed, test methods, and data reduction.

Nomenclature

A	cross-sectional area
ASC(-E2)	Advanced Stirling Convertor (second-generation engineering unit)
ASRG	Advanced Stirling Radioisotope Generator
CSAF	Cold Side Adapter Flange
DOE	Department of Energy
GRC	NASA Glenn Research Center
HT	high-temperature
IR	infrared
K	thermal conductivity
LM	Lockheed Martin
$\dot{Q}$	heat flow
$\dot{Q}_{conducting\,rod}$	heat flow through the conducting rod

$\dot{Q}_{env\,loss}$	heat lost to the environment
$\dot{Q}_{heater\,head}$	heat flow through the heater head
$\dot{Q}_{heater\,power}$	electrical power provided to the heater
$\dot{Q}_{HH\,insulation}$	heat flow through the insulation plug in the heater head
ΔT	change in temperature
TC	thermocouple
ΔX	change in location

1.0   Introduction

Accurately quantifying Stirling convertor efficiency and performance is important for designing the Advanced Stirling Radioisotope Generator (ASRG) and for mission planning. While electrical power output can be precisely quantified, thermal power input to the Stirling cycle cannot be directly measured. The past technique to estimate thermal power input to the convertor relies on accurately determining the environmental losses through the surrounding insulation of an operating convertor and subtracting these losses from the gross heat input (or electrical input) into the heat source. Traditionally, the environmental losses have been calculated and characterized based on testing a non-operating convertor. Using that characterization, the net heat input to the convertor has been calculated by subtracting the empirically modeled environmental losses from the measured heat source power. This method has previously worked well for convertors with lower operating temperatures and heaters that did not require some portion of the heater cartridge to be exposed to air. This technique did not characterize the system at the full heat flux and heat source temperature of an operating convertor and was suspected to contribute inaccuracies in performance and efficiency predictions. In an attempt to validate results from empirical models, a twofold path was taken to develop hardware capable of accurately imitating the thermal character of an operating and non-operating Advanced Stirling Convertors (ASC) without gas dynamics. The first path was to modify existing hardware, which enabled a quick turnaround and initiation of testing at the cost of an inaccurate representation of the thermal profile of an ASC. This path became known as the Mock Heater Head and is the focus of this paper. The second path was to develop higher fidelity hardware which could accurately simulate the thermal profile of an operating ASC. Convertor aspects, such as heat transfer area, lengths, diameters, material conductivity, and heat transfer paths were optimized to give the most accurate thermal profile possible. The second path became known as the Thermal Standard.

The Mock Heater Head was developed as a test unit to help better understand the environmental losses through the insulation package used while operating ASC in air. A key component to the design of the Mock Heater Head is a removable rod that mates to the interior dome of the heat head. Its purpose is to provide a conductive path representative of the heat input into the Stirling cycle. Two different conducting rods made of GRCop-84 and nickel were used to vary the thermal load and subsequently increase the thermal load on the heater. The Mock Heater Head test was utilized to investigate GRCop-84, which is a ternary Cu-Cr-Nb alloy developed at NASA GRC for high heat flux, high temperature applications, as a potential material for the conducting rod in the Thermal Standard. The copper material, GRCop-84, was selected as a candidate because of its high thermal conductivity (80 percent of pure copper) and ability to maintain yield strength greater than 100 MPa at temperatures up to 900 °C (Ref. 1). Also, nickel plating was applied to the GRCop-84 rod and tested as protection against oxidation at elevated temperatures.

While the physics presented in this paper hold true for the Mock Heater Head, a one-to-one comparison of the Mock Heater Head test results to the ASC-E2 convertor test results should not be made because the differences in head geometry and conductivity. Rather, performing various tests with the Mock Heater Head 1) gave insight into materials and coating selection for the conducting rod, 2) identified important design considerations for mounting, assembly, and accurate heat flow paths, and 3) verified test methods and data analysis techniques. This paper outlines the Mock Heater Head test

configuration, instrumentation, calculations performed, testing, and results, while presenting its usefulness as a pathfinder for the Thermal Standard.

2.0   Test Configuration

The test station for the Mock Heater Head is shown in Figure 1 along with a completed section view of the assembly. Note that the section view does not show the copper cooling coils that reject heat from the conducting rod or the Viton tubing that connects the cooling loops for the cold side adapter flange (CSAF) and conducting rod to the circulators, nor does it show the Kaowool blanket insulation that fills the voids inside the insulation housing and insulates the exposed portions of the conducting rod. The components inside of the insulation housing shown in Figure 1 relied on a preload rather than fasteners to affix the heater head to the CSAF and the heat source to the heater head. The CSAF was fastened to the bulk head and carried the mechanical load transferred through the other components. The thin wall of the Mock Heater Head was mated to a locating spotface on the CSAF and fixed through compression. Depending on the test, either an insulating thermal barrier made of ceramic paper or an alumina disk (further explanation will be given later) was placed between the heat source and heat collector plate. The heat source was concentrically located on top of the heater head with a button on the heater head that fits into the heat source. A preload stud was fit into the heat source and connected to a spring loaded plate attached to the top plate of the insulation housing. The insulation housing was held in tension from the preload and maintained static equilibrium of the system. The interior void of the heater head was filled with Kaowool blanket insulation as shown in Figure 1 except for a volume in the center for the conducting rod. The nickel rod mated to the interior dome of the heater head with a very thin piece of ceramic paper (0.178 mm thick) sandwiched in between and held in place with a preload. After operation with the nickel rod, oxidation on the interior dome of the head served as a diffusion barrier for the GRCop-84 rod and therefore, ceramic paper was not used. When a conducting rod was not used, its void was filled with Kaowool insulation.
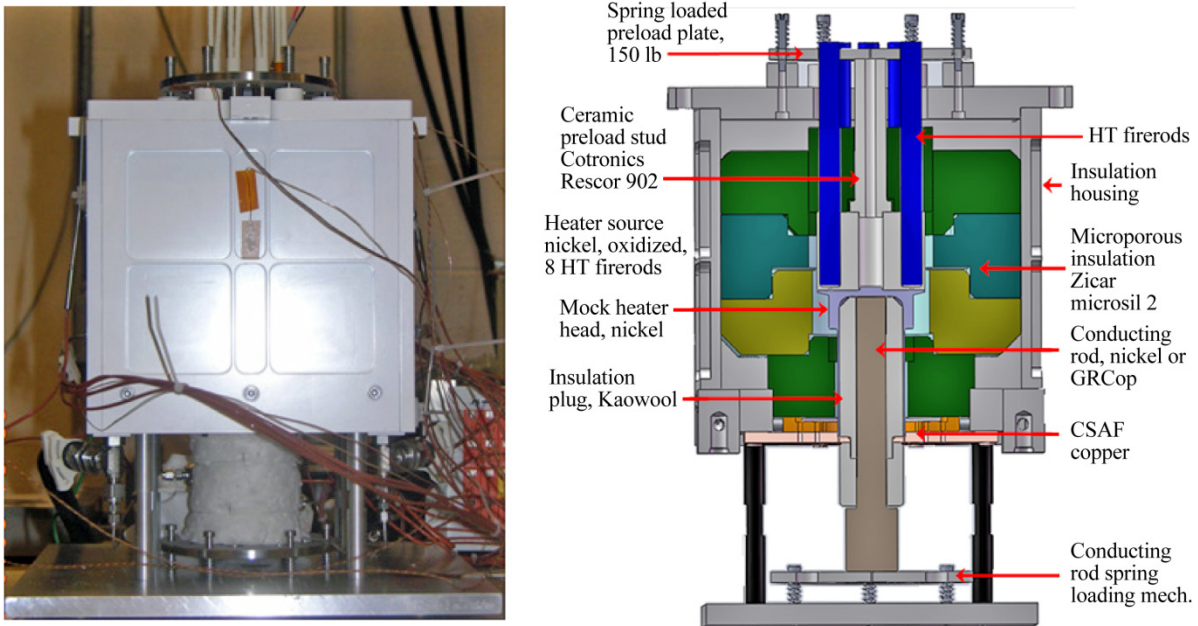

Figure 1.—Completed Mock Heater Head assembly ready for operation (left) and mechanical hardware section view (right).

The Mock Heater Head was adapted from a test heater head previously designed and fabricated to be used in testing a heat flux sensor. The original heater head was constructed from a solid piece of nickel 201 and matched a production heater head only in its heat collector interface plate and thermal mass. Its design intent was to flow a similar amount of energy to an operating convertor through the head to a rejection loop, but not to match exact geometry. Modifications for the Mock Heater Head did not match production geometry nor did it match thermal mass. The design intent was to conduct 110 W through the wall of the head and an additional 90 W through a nickel conducting rod that interfaced the heater head dome. The resulting 200 W would be representative of the energy rejected at the cold end of the convertor. A second rod made of GRCop-84 was designed to conduct 230 W with the intent that the incremental increases in thermal loading of the two rods would serve to quantify changes in the environmental losses.

3.0   Instrumentation

The Mock Heater Head, conducting rods, surrounding insulation, and insulation housing were instrumented with numerous thermocouples. Figure 2 shows a map of the thermocouples (TCs) in their approximate locations on a cross-sectional view of the hardware. Not including the TCs on the conducting rods, there were a total of thirty-three TCs used: sixteen 0.032–in. Type-N TC probes, three 0.020–in. Type-N TC probes, and fourteen Type-K surface mount TCs. Also, a Fluke i45 Infrared (IR) camera was used to measure temperatures on the exposed high-temperature (HT) firerod leads.

The Mock Heater Head was instrumented with seven thermocouples, as shown in Figure 3. There were four located 90° apart radially at a location 8.00 mm from the heat collector face. An additional three TCs were added in line along the axial length of the smaller diameter portion of the heater head. The locations of these TCs were measured from the cold side of the heater head and their measurements were 10.7, 36.6, and 67.7 mm.

The nickel 201 conducting rod was instrumented with four 0.032–in. Type-N thermocouples. The TCs were mounted to the surface of the rod using Inconel band straps that were spotwelded to the nickel rod. The TCs were mounted in-line along the length of the rod, and their locations measured from the smaller diameter end interfacing the hot-end of the heater head were 26.4, 50.0, 76.2, and 101.6 mm. These TCs were necessary for the calculation of the heat rejected through the conducting rod and the estimated environmental losses, which will be described in detail later.
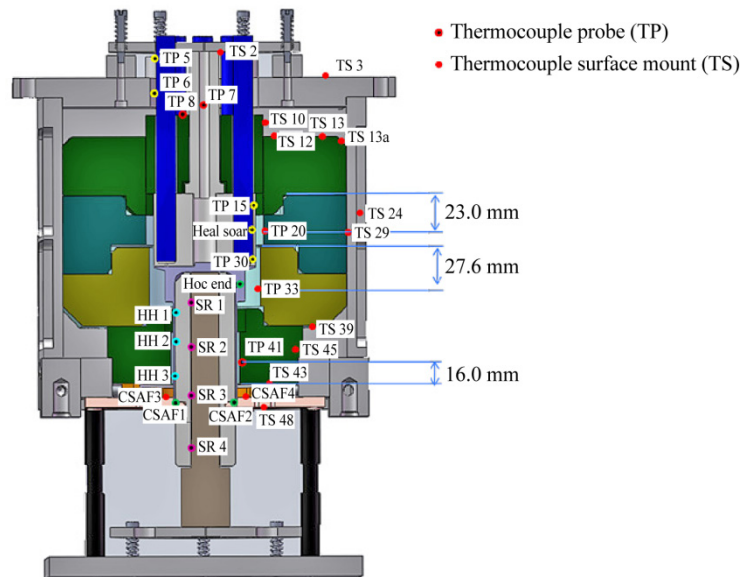

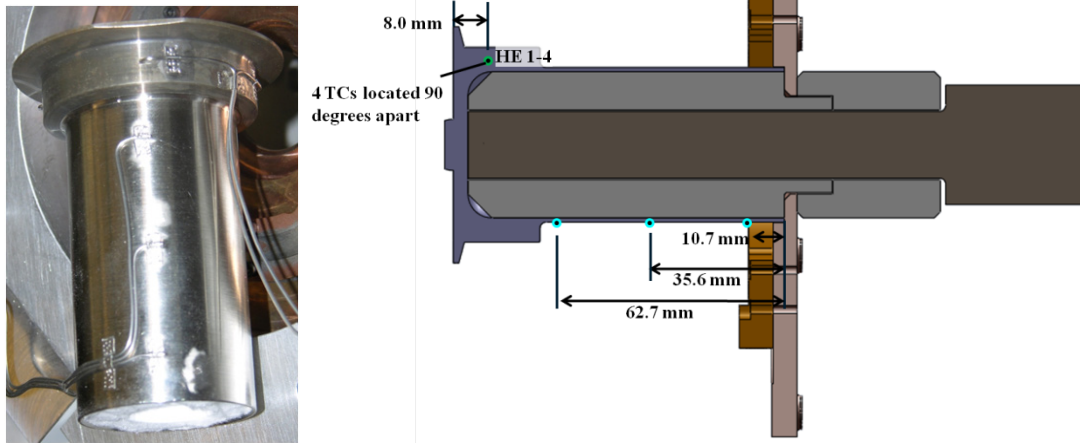Figure 2.—Thermocouple locations for the Mock Heater Head test setup.

Figure 3.—Thermocouple instrumentation on the Mock Heater Head (left) and cross-sectional view with dimensions (right).

Figure 4.—Thermocouple instrumentation on the GRCop-84 conducting rod.

The nickel-plated GRCop-84 conducting rod was instrumented with five 0.020–in. Type-N thermocouples. The TCs were mounted to the surface of the rod using 0.010–in. steel band straps that were spotwelded to the nickel plating. Initially, there was an attempt to use Inconel straps, but even at high levels of current, the spotwelder did not work. The TCs were mounted in-line along the length of the rod, and their locations measured from the smaller diameter end interfacing the hot-end of the heater head were 6.3, 12.5, 25.3, 63.1, and 101.3 mm, as seen in Figure 4. These TCs were also used to calculate the heat rejected through the conducting rod for the estimation of the environmental losses.

4.0 Testing

A series of tests were performed using the Mock Heater Head to accurately represent standard testing performed at GRC using an ASC-E2 convertor. An ASC-E2 convertor typically undergoes an insulation thermal loss characterization, during which the convertor does not operate, and then operates through a series of test points representative of anticipated mission conditions. In practice, two variations of insulation thermal loss characterization have been performed. One in which ceramic paper disks were placed between the heat source and the heater head to act as a thermal barrier. The intent of using the thermal barrier was to increase the temperature difference between to the heater head and the heat source to be more representative of temperatures observed during convertor operation. The second variation involves an alumina disk placed between the heat source and the heater head, which prevents the heat source from diffusion bonding to the heater head. Both of these insulation thermal loss characterization tests were performed using the Mock Heater Head, where the non-operating convertor was represented by not installing a conducting rod. An operating convertor was represented by testing with each of the two

conducting rods. The two rods had different thermal conductivities and were therefore representative of varying the piston amplitude in a Stirling convertor. For each of the four test cases described above, a test matrix consisting of four points was performed and is summarized in Table I. Additionally, tests were also performed to investigate the potential for ambient conditions (forced convection) and orientation to affect environmental losses, and are discussed in greater detail in the results section. In total five tests were performed, as summarized in Table II under the Results section. All tests were conducted by controlling the heat source temperature. The heat source temperature is normally the controlled parameter in a thermal loss test using a thermal barrier on an actual convertor, and since the thermal barrier test was the first performed, this approach was adopted for the remainder of Mock Heater Head testing. Therefore, for an equivalent heat source temperature, the hot-end temperature decreased for all simulated operating points. As a result of our experience with the Mock Heater Head, it was determined that it would be better to control hot-end temperature in Thermal Standard testing (because the control parameter in convertor testing is the hot end) to more easily show that the environmental loss increases as the heat source and/or hot end temperatures increase. For each steady-state test point, a 5-min average of heater power, current and voltage, and all temperature data were collected. In addition, an infrared photograph of the exposed HT firerod leads was taken.

TABLE I.—TEST MATRIX

Point	Heat source temperature (°C)	CSAF temperature (°C)
1	960	52
2	860	52
3	750	52
4	600	52

5.0   Calculations

All calculations served the end goal of determining the environmental losses for various test conditions. A comparison of the environmental losses gave insight into the sensitivity of environmental losses to changes in the thermal gradient as a result of increased thermal loading. The key calculations were heater head conduction, rod conduction, and conduction through the insulation inside the heater head. The summation of these calculations gives the cold-end losses and when subtracted from the heater power gives the environmental losses as shown in Eq. (1).

$$\dot{Q}_{env\,loss} = \dot{Q}_{heater\,power} - \left(\dot{Q}_{heater\,head} + \dot{Q}_{conducting\,rod} + \dot{Q}_{HH\,insulation}\right) \qquad (1)$$

The heater power was directly measured using a Yokogawa WT230 powermeter. Conduction through the heater head, conducting rod, and heater head insulation was calculated using Fourier's law in Eq. (2).

$$\dot{Q} = KA\frac{\Delta T}{\Delta X} \qquad (2)$$

The thermal conductivities used in the calculations were manufacturer values chosen from a temperature-dependent function based on the average temperature. The temperature-dependent thermal conductivities are shown in Figure 7 to Figure 9 in the Appendix. The cross-sectional areas used in the calculations were 143.9 mm^2 for the heater head, 938.1 mm^2 for the Kaowool insulation, 248.4 mm^2 for the nickel rod, and 214.2 mm^2 for the GRCop-84 rod. The temperatures used in the heater head calculation were taken from the 1st and 3rd TCs on the smaller diameter portion of the heater head, and the length between them was 53.3 mm. The temperatures used in the Kaowool calculation were an average of the four hot-end TCs on the heater head and an average of the two CSAF TCs. The length between them was 80.0 mm. The temperatures used in the nickel rod calculation were taken from the first and third TCs in reference from

the hot-end of the rod, and the length between them was 49.8 mm. Lastly, the temperatures used in the GRCop-84 rod calculation were taken from the 1st and 5th TCs in reference from the hot-end of the rod, and the length between them was 95.0 mm.

6.0   Results

Table II summarizes all tests in the sequence performed and includes key measured and calculated data for point 1 from Table I. Also, Figure 5 graphically shows a comparison of environmental losses to heat source temperature for all tests performed.

TABLE II.—SUMMARY OF TEST PERFORMED ON THE MOCK HEATER HEAD

Test	Interface between heat source and hot end	Conducting rod	Additional variable	Heat source temperature (°C)	Hot-end Temperature (°C)	Cold end loss (W)	Environmental loss (W)
1	Thermal Barrier	None		959	892	96	149
2	Alumina disk	Nickel Rod		960	915	167	148
3	Alumina disk	Nickel Rod	Forced Convection	959	915	166	164
4	Alumina disk	none		958	922	98	146
5	Alumina disk	GRCop-84 Rod		956	861	314	125

It was expected that the environmental losses would show a substantial increase in Test 2 and Test 5 where a conducting rod was installed when compared to the Test 1 and Test 4 where a rod was not installed. Rather, the trends showed that the environmental losses decreased when a greater thermal load was applied to the heat source via the conducting rods. In comparing Test 4 to Test 5 in Figure 5, the environmental losses decrease by 21 W as a result of installing the GRCop-84 rod. This phenomenon is most likely the result of the 61 °C drop in hot-end temperature. One might also expect a similar, yet smaller, decrease in hot-end temperature when the nickel rod was installed, but the hot-end temperature only dropped 7 °C in this case, making the change in environmental losses nearly indistinguishable from the other test points without a rod installed. This phenomenon is believed to be the result of the differences in heat transfer paths on the Mock Heater Head compared to an actual convertor. In the Mock Heater Head the conducting rod directly interfaced to the dome of the heater head, which acted as a direct heat sink to the heat source and varied the thermal gradients in a manner that was not desirable for comparison to convertor data. These results drove an effort for accurate heat flow paths in the Thermal Standard.

Test 3, which is represented by a single, worst case point in Figure 5, was performed to further investigate the affect of ambient conditions on environmental losses. This test involved using a Multicomp (Model: MC1123HST) fan placed at four distances from the HT Firerod leads to induce varying intensities of forced convection. A thermal anemometer was used to estimate the air velocity at the lead wires for each case, and an observed average value was recorded. Table III summarizes distance, air velocity, and gross heat input measurements during Test 5, and Figure 6 shows the observed relationship to air velocity. The thermal anemometer measurements are representative of velocities experienced at a location approximately 25 mm from the heater lead wires and in the path between the fan and wires. At ambient conditions, which are represented as an infinite distance in Table III, the approximate measured air velocity was 0.1 m/s and the gross heat input was 321.5 W. This point served as a baseline for comparison to the other points, with "Additional Heat Input," shown in Figure 6, being defined as the difference in gross heat input between any point and the baseline. As the fan was positioned closer to the exposed heater cartridges and lead wires, the heater worked harder to maintain temperature as a result of the increased convection. At some location between fan positions of 203 mm (3.5 m/s) and 559 mm (1.0 m/s), additional air flow appeared to have limited effect on the gross heat input. For this reason, the trend shown in Figure 6 is truncated. The phenomenon of increased flow

approaching a limit in convective effects was expected, but not further investigated for the determination of that transition point. The results and trends of this test should be used as reference for gaining a better understanding of the heat source losses under different environmental conditions.

Other air velocity measurements were also made near the test article. A measurement taken directly below the air conditioning vent, which is at a distance of approximately 1.5 m from the test article and does not blow directly toward the test article, had an output velocity of 1.5 m/s. Other measurements taken in the general vicinity of the test article without operation of the fan never exceeded 0.2 m/s. For this particular test, it is unlikely that forced convection changes affected the gross heat input by more than ±1.1 W.

Mock Heater Head Test Results

Figure 5.—Summary of environmental losses versus heat source temperature for tests performed.

TABLE III.—AIR VELOCITY MEASUREMENTS FROM THE FORCED CONVECTION INVESTIGATION

Distance (mm)	Air velocity (m/s)	Gross heat input (W)
∞	0.1	321.5
1,626	0.4	322.6
965	0.9	327.5
559	1.0	330.1
203	3.5	339.3

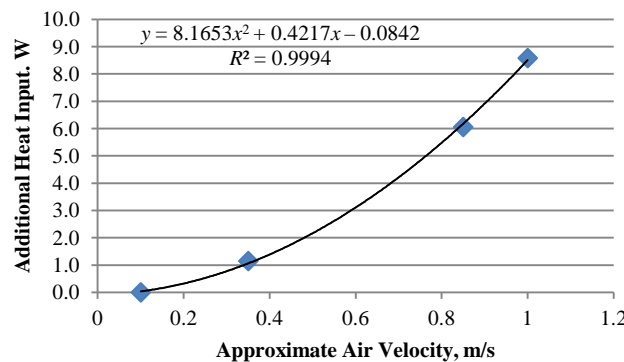$$y = 8.1653x^2 + 0.4217x - 0.0842$$
$$R^2 = 0.9994$$

Figure 6.—Additional heat input as a function of air velocity.

7.0 Conclusions

The need to flow heat through the validation hardware much like an operating ASC was determined to be a requirement for this validation effort because the Mock Heater Head did not result in a thermal profile adequate for use in validating empirical and numerical models. That being said, the Mock Heater Head test served as a pathfinder for selection of the following items for the Thermal Standard test: verifying materials used for the conducting Rod, identifying design features for the heat collector and CSAF, identifying instrumentation locations for calculating heat conducted to the cold end, designing the heat rejection system mounting method for ease of disassembly and shipment, and identifying preferred test methods used for characterization such as how to control the heat input. The GRCop-84 material was identified as having superior strength at expected test temperatures, and nickel plating was found to be suitable for protecting the copper rod from oxidation during the test. Additionally, diffusion bonding between the rod and heater head was prevented by installing a thin layer of Cotronics ceramic paper between the heater block and head. Lastly, the Mock Heater Head test verified the methodology and use of an IR camera to measure temperatures on the exposed surfaces of the heat source, namely the HT firerod leads for input into a thermal model.

In addition to this paper, three other papers have been written to explain the work performed in the effort to accurately determine the environmental losses through the surrounding insulation of an operating convertor and quantify Stirling convertor performance and efficiency. This paper has described the first step in a process that has directly played a role in the successful testing of the Thermal Standard validation hardware, described in the paper titled, "Evaluation of Advanced Stirling Convertor Net Heat Input Correlation Methods using a Thermal Standard," (Ref. 2) as well as the successful validation of the computation model described in the paper titled, "A Computational Methodology for Simulating Thermal Loss Testing of the Advanced Stirling Convertor" (Ref. 3). A final paper titled, "Overview of Heat Addition and Efficiency Predictions for an Advanced Stirling Convertor," (Ref. 4) provides an overview of the entire effort.

Appendix

Figure 7 to Figure 9 show the thermal conductivities of nickel 201, Kaowool, and GRCop-84, respectively.
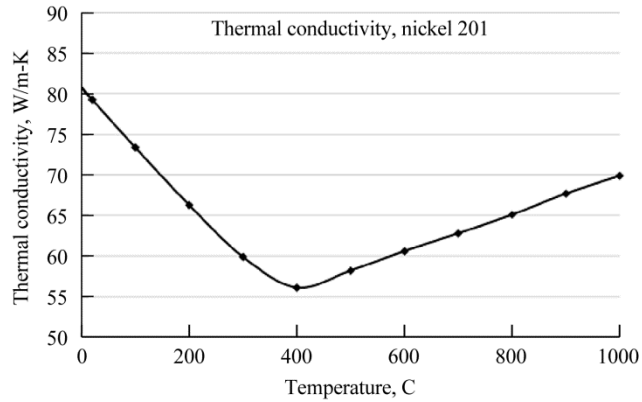

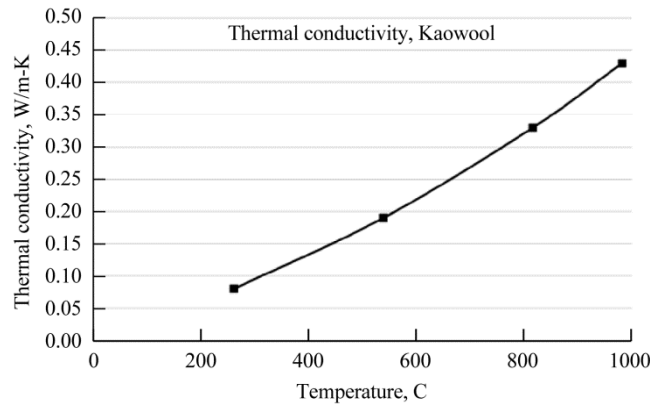Figure 7.—Manufacturer's thermal conductivity of nickel 201 (Ref. 5).

Figure 8.—Manufacturer's thermal conductivity of Kaowool (Ref. 6).
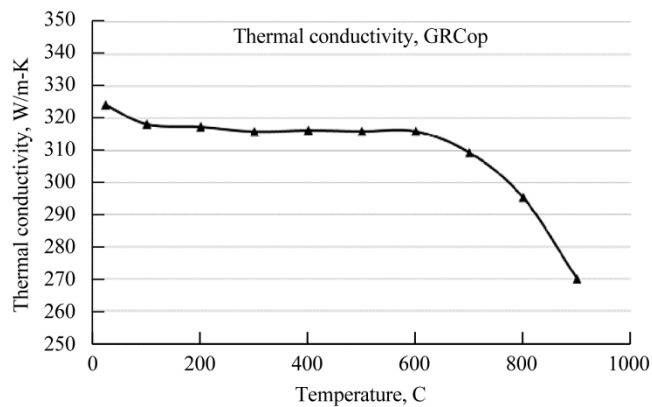

Figure 9.—Thermal conductivity of GRCop-84 (Ref. 7).

References

1. Ellis, David L., "GRCop-84: A High-Temperature Copper Alloy for High-Heat-Flux Applications", NASA/TM—2005-213566, 2005.
2. Briggs, M.H., "Evaluation of Advanced Stirling Convertor Net Heat Input Correlation Methods using a Thermal Standard," Proceedings of the Ninth International Energy Conversion Engineering Conference (IECEC 2011) American Institute for Aeronautics and Astronautics, 2011.
3. Reid, T.V., "A Computational Methodology for Simulating Thermal Loss Testing of the Advanced Stirling Convertor," Proceedings of the Ninth International Energy Conversion Engineering Conference (IECEC 2011) American Institute for Aeronautics and Astronautics, 2011.
4. Wilson, S.D., "Overview of Heat Addition and Efficiency Predictions for an Advanced Stirling Convertor," Proceedings of the Ninth International Energy Conversion Engineering Conference (IECEC 2011) American Institute for Aeronautics and Astronautics, 2011.
5. "Nickel 200 & 201," Specialty Metals [online technical bulletin], URL: http://www.specialmetals.com/documents/Nickel%20200%20&%20201.pdf [cited 14 July 2011].
6. "Thermal Ceramics – Blanket Products," Thermal Ceramics [online technical bulletin], URL: http://www.barteltinsulation.com/pdfs/CERAMICBLANKET.pdf [cited 14 July 2011].
7. Thermophysical Properties Research Laboratory Inc. Report #4629 November 2010.

1. REPORT DATE *(DD-MM-YYYY)*
01-01-2012

2. REPORT TYPE
Technical Memorandum

3. DATES COVERED *(From - To)*

4. TITLE AND SUBTITLE
Environmental Loss Characterization of an Advanced Stirling Convertor (ASC-E2) Insulation Package Using a Mock Heater Head

5a. CONTRACT NUMBER

5b. GRANT NUMBER

5c. PROGRAM ELEMENT NUMBER

6. AUTHOR(S)
Schifer, Nicholas, A.; Briggs, Maxwell, H.

5d. PROJECT NUMBER

5e. TASK NUMBER

5f. WORK UNIT NUMBER
WBS 138494.05.02.04.03

7. PERFORMING ORGANIZATION NAME(S) AND ADDRESS(ES)
National Aeronautics and Space Administration
John H. Glenn Research Center at Lewis Field
Cleveland, Ohio 44135-3191

8. PERFORMING ORGANIZATION REPORT NUMBER
E-17827

9. SPONSORING/MONITORING AGENCY NAME(S) AND ADDRESS(ES)
National Aeronautics and Space Administration
Washington, DC 20546-0001

10. SPONSORING/MONITOR'S ACRONYM(S)
NASA

11. SPONSORING/MONITORING REPORT NUMBER
NASA/TM-2012-217291

12. DISTRIBUTION/AVAILABILITY STATEMENT
Unclassified-Unlimited
Subject Category: 20
Available electronically at http://www.sti.nasa.gov
This publication is available from the NASA Center for AeroSpace Information, 443-757-5802

13. SUPPLEMENTARY NOTES

14. ABSTRACT
The U.S. Department of Energy (DOE) and Lockheed Martin Space Systems Company (LMSSC) have been developing the Advanced Stirling Radioisotope Generator (ASRG) for use as a power system for space science missions. This generator would use two high-efficiency Advanced Stirling Convertors (ASCs), developed by Sunpower Inc. and NASA Glenn Research Center (GRC). As part of ground testing of these ASCs, different operating conditions are used to simulate expected mission conditions. These conditions require achieving a specified electrical power output for a given net heat input. While electrical power output can be precisely quantified, thermal power input to the Stirling cycle cannot be directly measured. In an effort to improve net heat input predictions, the Mock Heater Head was developed with the same relative thermal paths as a convertor using a conducting rod to represent the Stirling cycle and tested to provide a direct comparison to numerical and empirical models used to predict convertor net heat input. The Mock Heater Head also served as the pathfinder for a higher fidelity version of validation test hardware, known as the Thermal Standard. This paper describes how the Mock Heater Head was tested and utilized to validate a process for the Thermal Standard.

15. SUBJECT TERMS
Stirling; Net heat input; Insulation loss; Environmental loss; Thermal loss

16. SECURITY CLASSIFICATION OF:

a. REPORT
U

b. ABSTRACT
U

c. THIS PAGE
U

17. LIMITATION OF ABSTRACT
UU

18. NUMBER OF PAGES
20

19a. NAME OF RESPONSIBLE PERSON
STI Help Desk (email:help@sti.nasa.gov)

19b. TELEPHONE NUMBER *(include area code)*
443-757-5802